

Supporting Information

Ice Recrystallization Inhibition Mechanism of Zwitterionic Poly (carboxybetaine methacrylate)

Yanfang Chen^{a,b,#}, *Xiaojie Sui*^{c,#}, *Tiantong Zhang*^{a,b}, *Jing Yang*^{a,d}, *Lei Zhang*^{a,d,*},
You Han^{a,b,*}

^a School of Chemical Engineering and Technology, Tianjin University, Tianjin 300072,
China

^b Haihe Laboratory of Sustainable Chemical Transformations, Tianjin 300192, China

^c School of Life Science, Zhengzhou University, 100 Science Road, Zhengzhou
450001, PR China

^d Department of Biochemical Engineering, Frontier Science Center for Synthetic
Biology and Key Laboratory of Systems Bioengineering (MOE), School of Chemical
Engineering and Technology, Tianjin University, Tianjin, 300072, China.

The first two authors contributed equally to this work.

* Corresponding authors: You Han, yhan@tju.edu.cn

[Lei Zhang, lei_zhang@tju.edu.cn](mailto:lei_zhang@tju.edu.cn)

Table of Contents

1. Materials and Methods	S3-S4
Synthesis of carboxybetaine polymers	S3
Ice recrystallization inhibition (IRI) analysis	S3
2. Computational Methods	S4-S6
Molecular dynamics simulations	S4-S6
3. Supplementary Tables	S7
Table S1: The concentration of PCBMA	S7
Table S2: GPC characterization of PCBMA	S7
Table S3: Types and numbers of molecules involved in simulation	S7
4. Supplementary Figures	S8-S15
Figure S1: ¹ H NMR spectra of CBMA in D ₂ O.	S8
Figure S2: Initial configuration of molecular dynamics simulation	S9
Figure S3: The Gibbs-Thomson effect of PCBMA ₃₀	S10
Figure S4: The Growth rate of ice in different systems	S11
Figure S5: Analysis of interaction energy between PCBMA and water	S12
Figure S6: Some PCBMA atoms embedded to ice lattices in x-y plane	S13
Figure S7: Some PCBMA atoms embedded to ice lattices in x-z plane	S13
Figure S8: Comparisons of MSD of water and PCBMA	S14
Figure S9: Different water behavior around PCBMA ₃₀ /PCBMA ₄₀	S15
5. Reference	S16

Materials and Methods

Synthesis of carboxybetaine polymers

Carboxybetaine methacrylate (CBMA) monomers were synthesized by the reaction of DMAEMA and β -propiolactone as previously reported¹. The carboxybetaine polymers (PCBMA) were synthesized by CBMA monomers using an atom transfer radical polymerization method². Firstly, CBMA (5 mmol) and DMF/water (volume ratio at 1:1, 10 mL) mixture were added into a Schlenk tube. Then, the solution was deoxygenized by with nitrogen for 30 min. Afterward, the EBiB, CuBr, Cu₂Br, bpy with a molar ration of 1:4:0.4:8.8 were added into the Schlenk tube under nitrogen protection. The solution was reacted at 25 °C for 24 h and the reaction was terminated by rapid cooling in an ice bath and exposure to air. The product PCBMA was purified by dialysis against deionized water using semi-permeable cellulose tubing with the molecular weight cut-off of 1000 Da, followed by lyophilization. By varying the molar ratio of CBMA/EBiB, PCBMA with different DP was obtained. The CBMA monomer was characterized by ¹H NMR (Figure S1) and the Gel permeation chromatography (GPC) analysis was performed to determine the M_w, M_n, DP and the polymer dispersity index (PDI) of the PCBMA (Table S2).

Ice recrystallization inhibition (IRI) analysis

The IRI analysis was performed using a splat cooling method as previously reported³. The PCBMA with different DP was dissolved in water with desired a fixed molar concentration of 1.77 mmol/L, which was corresponding to the concentration used in MD simulations. The concentrations of PCBMA can be seen in Table S1. A droplet of 10 μ L of the polymer solution was dropped onto the silicon wafer placed at the cryostage (FDCS 196, Linkam) with an initial temperature of -60 °C from 1.5 m height above it. The droplet froze immediately and formed a thin ice film. Afterward, the cryostage was heated to -8 °C at a rate of 5 °C/min and annealed at -8 °C for 30 min. During this period, the ice film was imaged by a digital camera (Nikon DS-Ri2) to monitor the size change of ice crystals. Ten largest ice crystals were selected in each

image and the largest length in any axis of the crystals was measured. The mean value of these ten ice crystals was determined as the mean largest grain size (MLGS). Each measurement was performed for three times. Smaller MLGS indicated stronger IRI activity of PCBMA polymers.

Computational Methods

Molecular dynamics simulations

Molecular dynamics (MD) simulations in this work were carried out using the step of 2 fs with Gromacs-2019.5⁴. The OPLS-AA force field with 1.20*CM5 atomic charge⁵ and TIP4P/Ice⁶ model were employed for PCBMA and water molecules, respectively. The simulations investigate the impact of polymerization degree on IRI activity. The selection of the initial structure of the PCBMA molecule is as follows: firstly, the PCBMA molecule was established by Material Studios software, then adjusting molecular structure using annealing cycles with cycle temperature 0 K to 500 K, the cycle time is 2ns, and 200ps is a cycle. The structure with the lowest potential energy was selected, placed in a water-filled box, and pre-equilibrated under the NPT ensemble for 20 ns at a temperature and pressure of 300 K and 1 bar, respectively. The pre-equilibrated macromolecules are extracted as the initial structure for simulating molecular dynamics, as shown in **Figure S2(b)**. Each kinetic simulation was run for 200 ns and the temperature was controlled at 265 K, which was consistent with the experiment. To avoid chance in a single simulation, three replicate experiments were run for each system.

After energy minimization and a 1.0 ns pre-nvt run, a 200 ns run with an integration step size of 2.0 fs was performed. The long-range electrostatic interaction was described by the Particle-Mesh Ewald (PME) method with the cutoff of 1.0 nm, and the same cutoff was used for the van der Waals interaction. When the distance exceeds 10 Å, the switching function kicks in, smoothly reducing electrostatic and van der Waals interactions to zero. The NVT ensemble was used in the simulation, and the v-rescale algorithm was used for temperature. where the x, y, and z lengths of the

simulated boxes fluctuate independently. Apply periodic boundary conditions to replicate the seed ice configuration periodically in the x-z plane. The LINCS algorithm constrains the intramolecular bonds of betaine or PCBMA molecules and water molecules.

In this study, we use the chain length of macromolecular PCBMA as the influencing factor to explore their effects on inhibiting the growth of ice crystals. The chain length is represented by the degree of polymerization. Considering that the length of the PCBMA will affect the size of the box in the simulation and thus the time required for the simulation, in this study, the maximum value of the degree of aggregation is chosen to be 40. To explore the effect of polymerization degree on inhibiting the growth of ice crystals, we selected PCBMA molecules with chain lengths of 10, 20, 30, and 40 for simulation.

In order to more accurately obtain the ice crystal growth trend and the effect of the above simulations on inhibiting ice crystal growth, we performed a set of simulations of pure water freezing as a control group.

Table S3 shows the number of each type of molecule placed in the box in this study. In this study, Ih ice crystals were selected and placed on the bottom layer, as shown in **Figure S2(c)**. An ice crystal contains 2304 water molecules, with a, b, c side lengths of 108.197, 7.810, and 88.32, respectively, which are fixed on the x-y surface and used as an ice seed for subsequent water growth on the ice layer (see **Figure S2(a)**).

In the 5 systems described above, the box size is the same in the control simulation process, which is 108.197, 88.32, 107.81. Above the ice species, there are a large number of water molecules. For different systems, the number of water molecules contained is different, but the difference is not large. The number of water molecules ranges from 29078 to 29623. Below the ice species and above the water molecules, there are vacuum layers of 1 nm each to facilitate the observation of subsequent simulation results. The distance between each PCBMA molecule and the ice surface is the same, which is controlled to be 10 angstroms.

The properties of PCBMA, e.g., mean square displacement (MSD), diffusion constant(D), and interaction energy with water, were analyzed based on the mentioned

simulation. Interestingly, PCBMA30 enters a horizontal state instead of a vertical state. To clarify the mechanism, we calculate the total energy of PCBMA30 at the different state in the ice growth system. The energy of the horizontal state was found to be lower, which means the horizontal state would be more stable in the ice phase.

MSD is a function of time, which measures the mean square of the amount of ion displacement over time t , and its definition is as follows:

$$MSD(t) = \langle |r(t) - r(0)|^2 \rangle \quad (1)$$

The diffusion constant (D), also known as the self-diffusion coefficient, can be obtained from MSD according to Einstein's formula.

$$3D = \lim_{t \rightarrow \infty} \frac{\langle |r(t) - r(0)|^2 \rangle}{2t} \quad (2)$$

It's really just a problem of calculating the slope, which is shorthand:

$$6D = \lim_{t \rightarrow \infty} \frac{MSD(t)}{t} \quad (3)$$

Supplementary Tables

Table S1. The concentration of PCBMA

	PCBMA10	PCBMA20	PCBMA30	PCBMA40
Molar concentration (mmol/L)	1.77	1.77	1.77	1.77
Mass Concentration (mg/mL)	4.05	8.10	12.15	16.24

Table S2. GPC characterization of PCBMA

Sample	Mw	PDI	DP
PCBMA10	3585	1.53	15
PCBMA20	7154	1.99	30
PCBMA30	10915	1.94	47
PCBMA40	13681	2.04	59

Table S3. Types and numbers of molecules involved in simulation

System	$N_{\text{Liquid Water}}$	N_{Ice}	N_{PCBMA}
Pure water	29623	1	0
Water+PCBMA10	29153	1	1 PCBMA10
Water+PCBMA20	29155	1	1 PCBMA20
Water+PCBMA30	29155	1	1 PCBMA30
Water+PCBMA40	29078	1	1 PCBMA40

Supplementary Figures

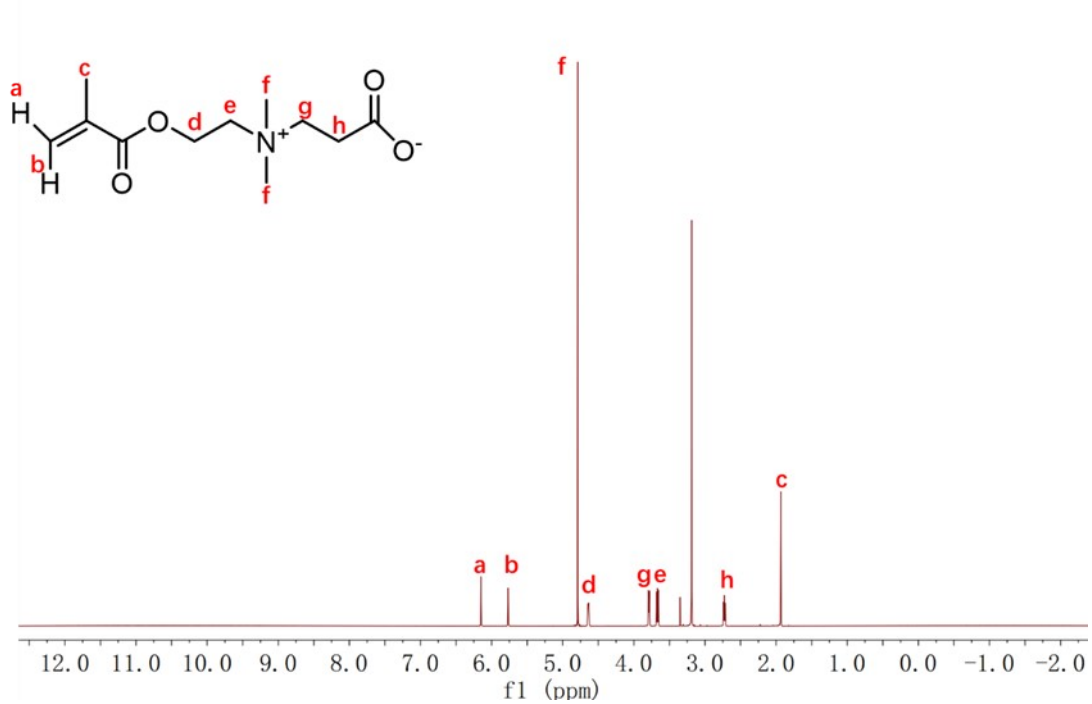


Figure S1. ¹H NMR spectra of CBMA in D₂O.

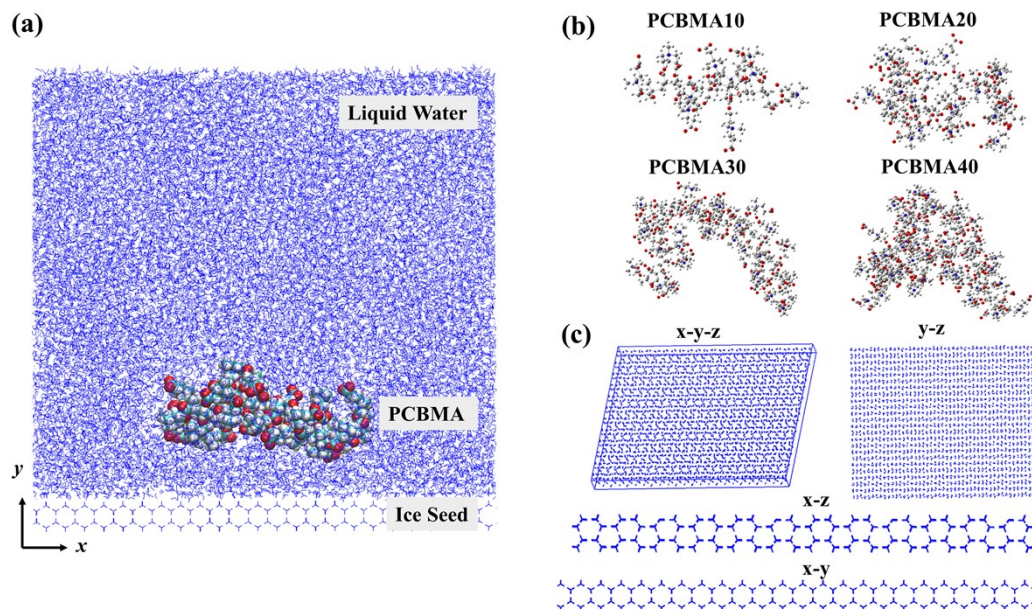


Figure S2. Initial configuration of molecular dynamics simulation. (a) PCBMA-Ice-Water Simulation System Viewed in the x-y-plane, in which PCBMA molecules are represented by VDW models. (b) The configuration of PCBMA. (c) The configuration of Ih ice species.

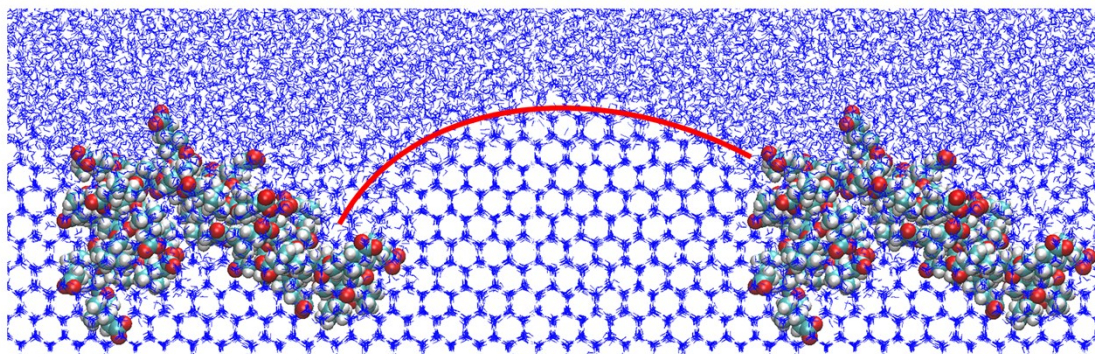


Figure S3. Schematic illustration of the Gibbs-Thomson effect due to the growth of ice crystals near PCBMA30 (x-y plane, time point: 100 ns). For a clear demonstration, concatenate two adjacent periodic images along the x-axis.

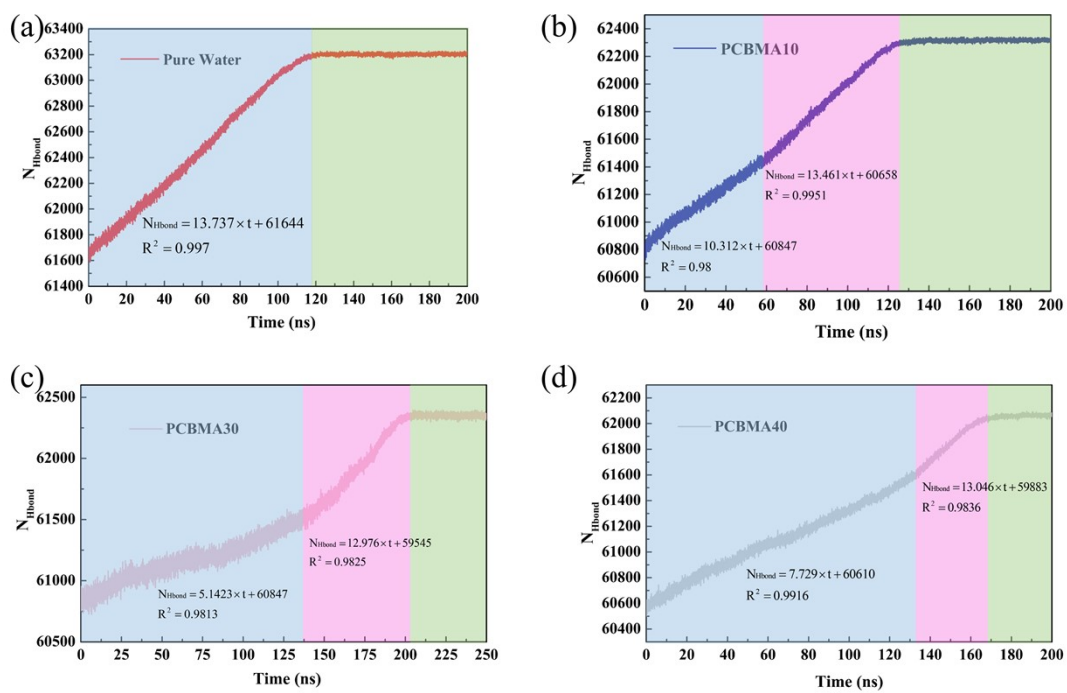


Figure S4. Analysis of ice crystal growth rate in pure water, PCBMA10, PCBMA30 and PCBMA40.

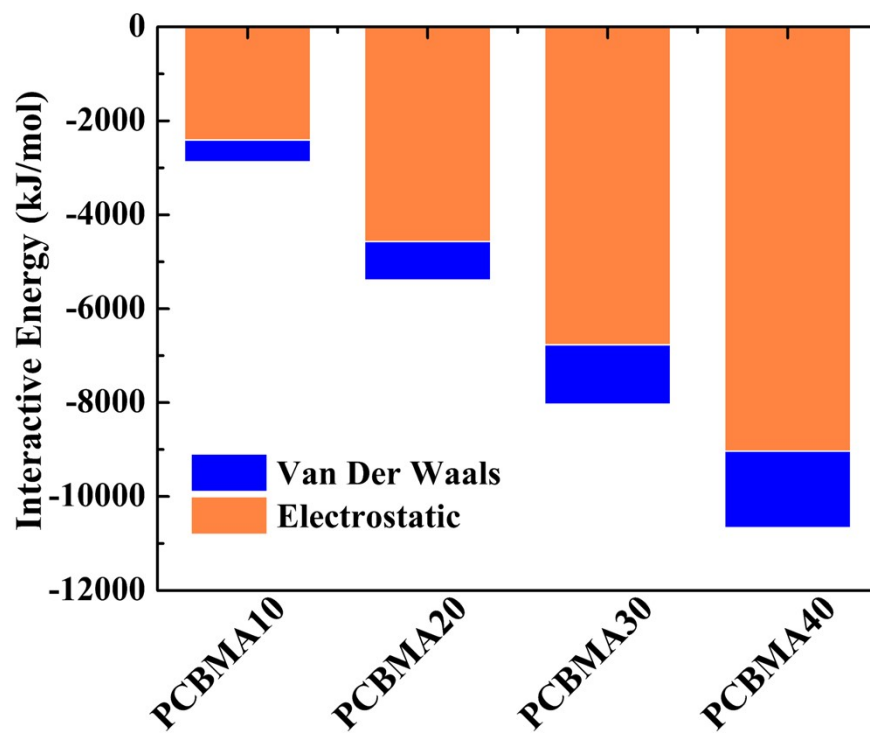


Figure S5. Analysis of interaction energy between PCBMA and water.

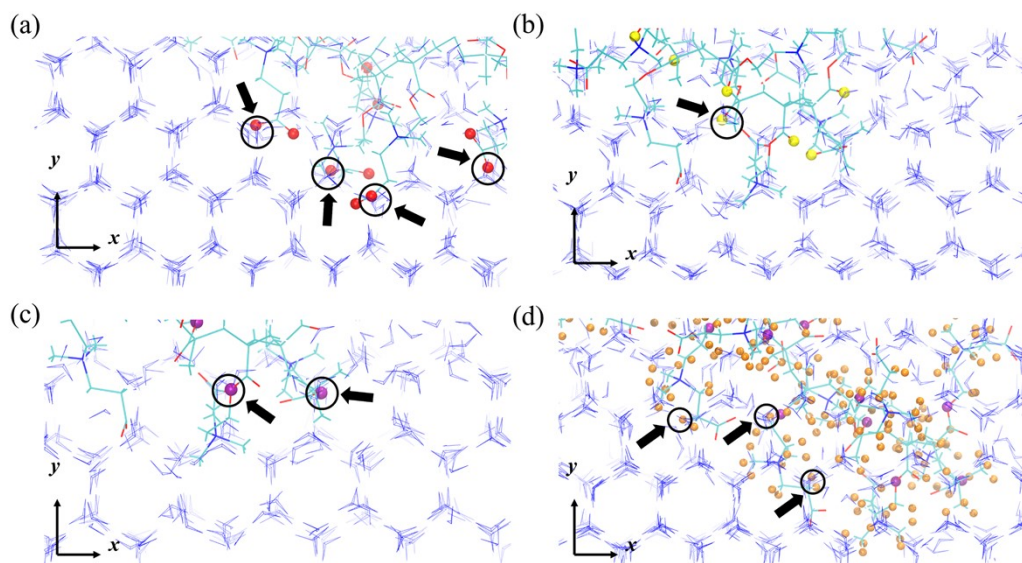


Figure S6. Some PCBMA atoms embedded to ice lattices in x-y plane.

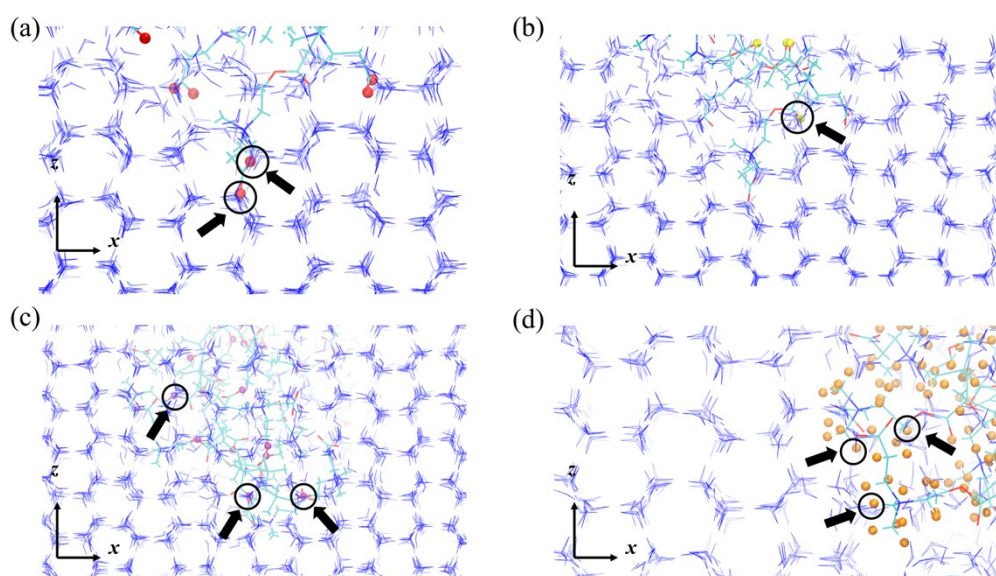


Figure S7. Some PCBMA atoms embedded to ice lattices in x-z plane.

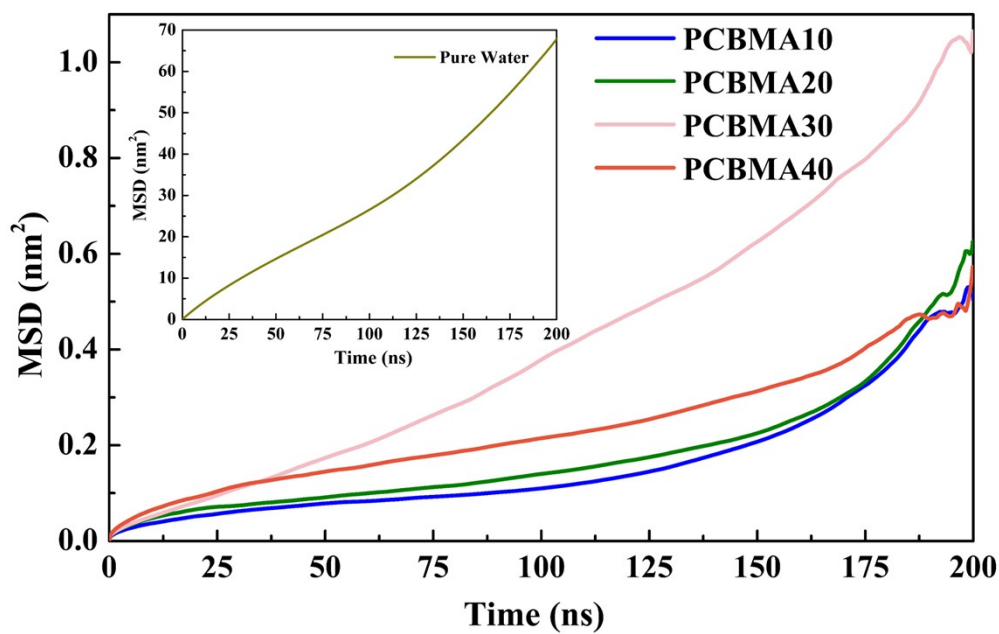


Figure S8. Comparison of mean square displacement (MSD) of water molecule and PCBMA molecule.

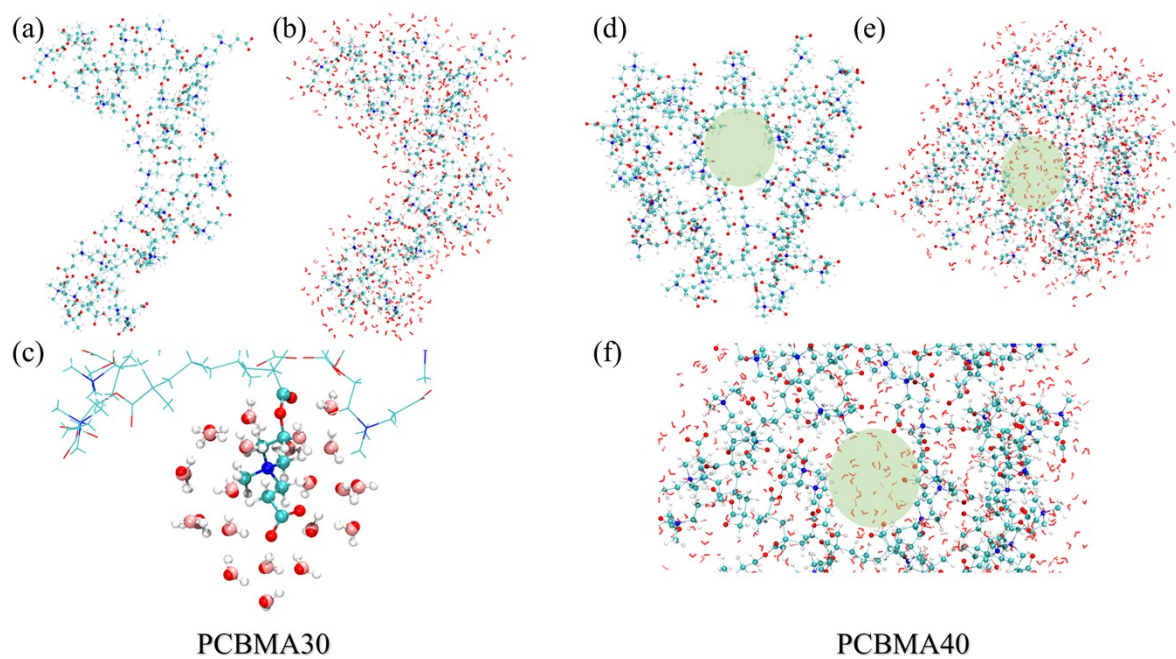


Figure S9. Comparison of water molecule behavior around PCBMA30 and PCBMA40.

References

- (1) Zhang Z, Chao T, Chen S, et al. Superlow fouling sulfobetaine and carboxybetaine polymers on glass slides[J]. *Langmuir*, **2006**, 22(24): 10072-10077.
- (2) Cheng G, Li G, Xue H, et al. Zwitterionic carboxybetaine polymer surfaces and their resistance to long-term biofilm formation[J]. *Biomaterials*, **2009**, 30(28): 5234-5240.
- (3) Bai G, Song Z, Geng H, et al. Oxidized quasi-carbon nitride quantum dots inhibit ice growth[J]. *Advanced Materials*, **2017**, 29(28): 1606843.
- (4) Abraham M J, Murtola T, Schulz R, et al. GROMACS: High performance molecular simulations through multi-level parallelism from laptops to supercomputers[J]. *SoftwareX*, **2015**, 1: 19-25.
- (5) Dodda, L. S., Vilseck, J. Z., Tirado-Rives, J. & Jorgensen, W. L. 1.14*CM1A-LBCC: Localized Bond-Charge Corrected CM1A Charges for Condensed-Phase Simulations. *J. Phys. Chem. B*.**2017**, 121, 3864-3870 .
- (6) Abascal, J. L. F., Sanz, E., García Fernández, R. & Vega, C. A potential model for the study of ices and amorphous water: TIP4P/Ice. *J. Chem. Phys.***2005**, 122, 234511 .